The Role of Angular Momentum in Fission

Ramona Vogt (LLNL & UC Davis)

Jorgen Randrup (LBNL)

LLNL-PRES-836355

This work performed under the auspices of the U.S. Department of Energy by Lawrence Livermore National Laboratory under Contract DE-AC52-07NA27344

Fission is a complicated process involving multiple scales

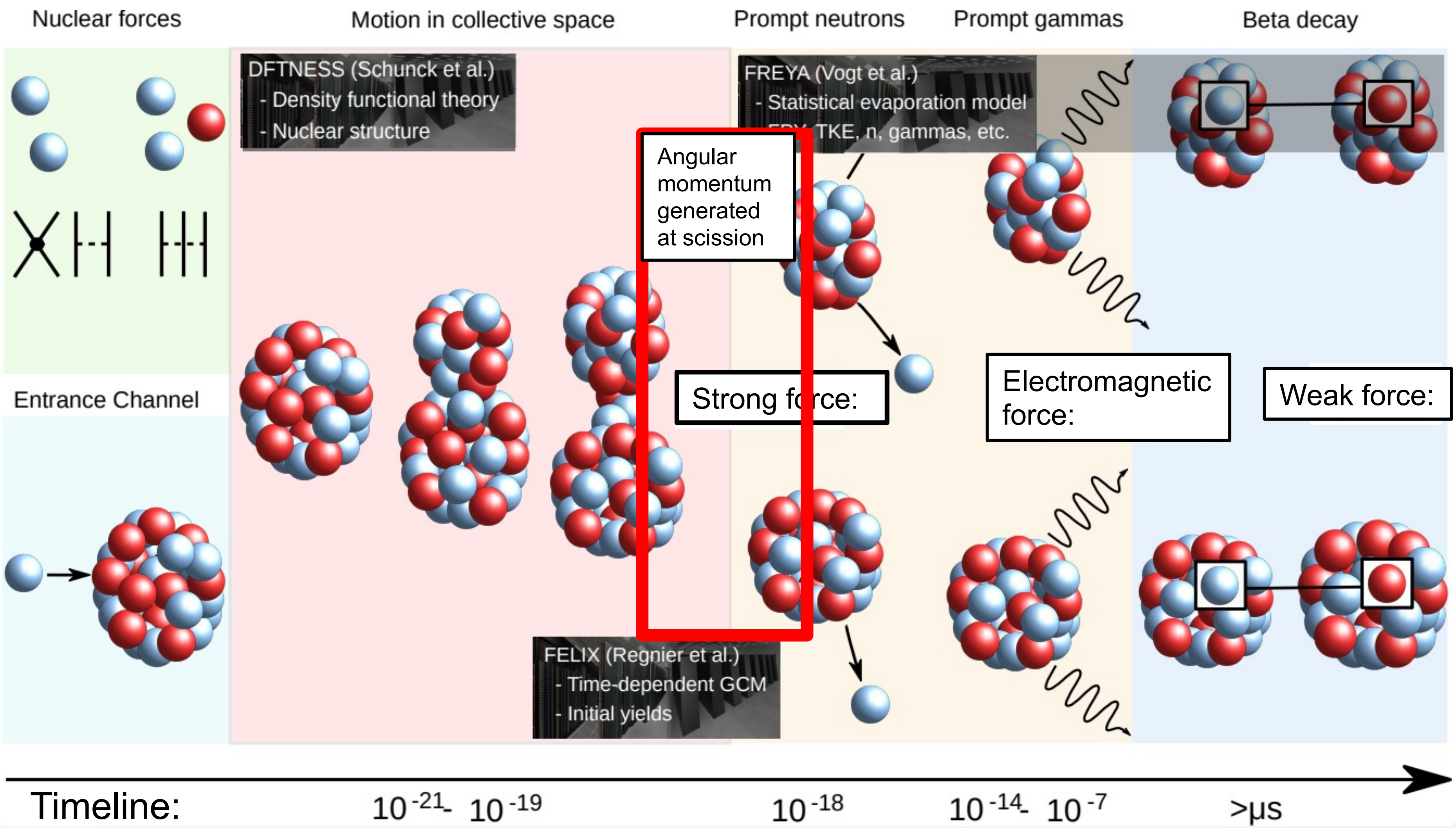

Specialized physics models required to study fission: phenomenology required to model complete events

We have been developing **FREYA** (Fission Reaction Event Yield Algorithm) since 2009 to study fission event-by-event

- First such fission model ever published and made generally available
- Showed the importance of energy and momentum conservation for understanding fission data
- **FREYA** is fast enough for users to study fission of different isotopes and energies in real time with a laptop – a big advantage (focus on **FREYA** here for simplicity)

Other codes similar in concept to **FREYA** have also appeared, differ in details:

- **CGMF**; **FIFRELIN**; **GEF**

Older codes deterministic, based on average events, tuned to subsets of average data

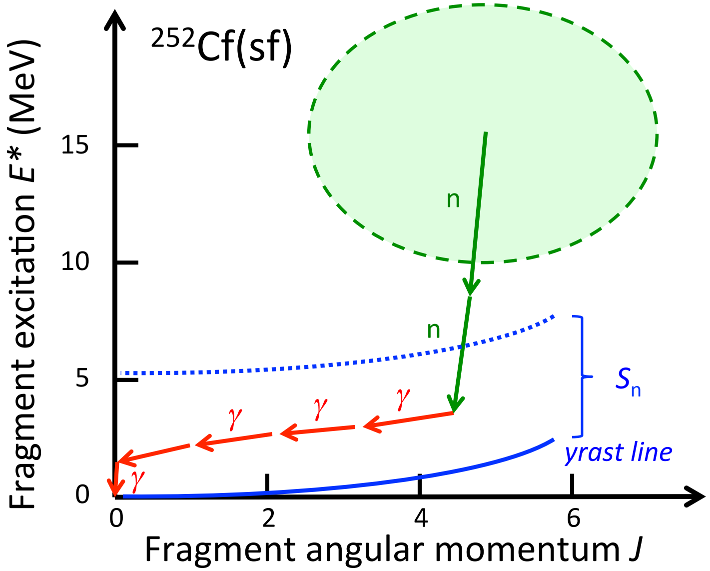

Event-by-event modeling is efficient framework for studying fission

Event-by-event (Monte Carlo) modeling has been used in high energy nuclear and particle physics when there are multiple outcomes – useful for studying detector response and predicting outcomes of experiment

Calculational framework easily adoptable for studying fission

Goal(s): *Fast* generation of (large) samples of complete fission events

Complete fission event: Full kinematic information on all final particles

Two product nuclei: $Z_H, A_H, \boldsymbol{P}_H$ and $Z_L, A_L, \boldsymbol{P}_L$

ν neutrons: $\{ \boldsymbol{p}_n \}$, $n = 1,\ldots,\nu$

N_γ photons: $\{ \boldsymbol{p}_m \}$, $m = 1,\ldots,N_\gamma$

Advantage of having *samples* of complete events:

Straightforward to extract *any* observable, including fluctuations and correlations, and to take account of cuts & acceptances

Advantage of *fast* event generation:

Can be incorporated into transport codes

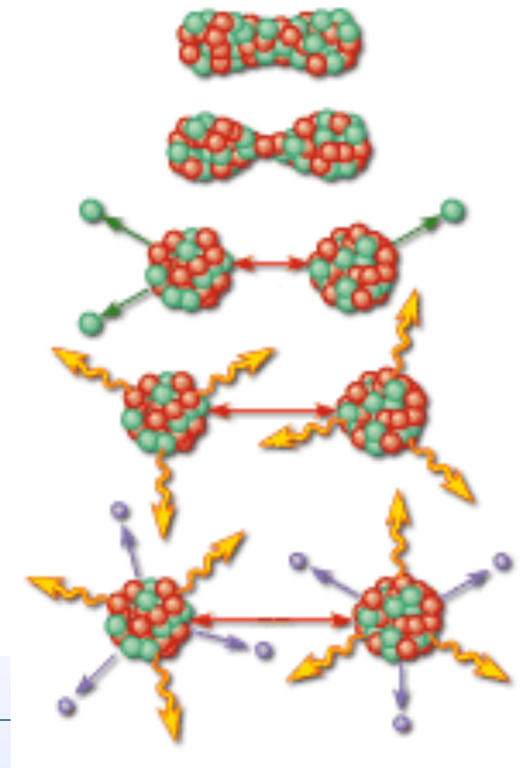

Every part of a fission event is correlated

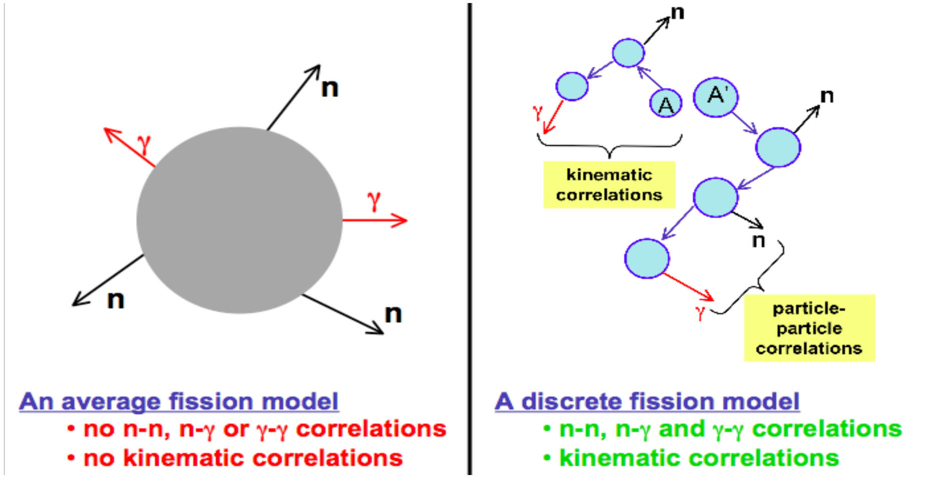

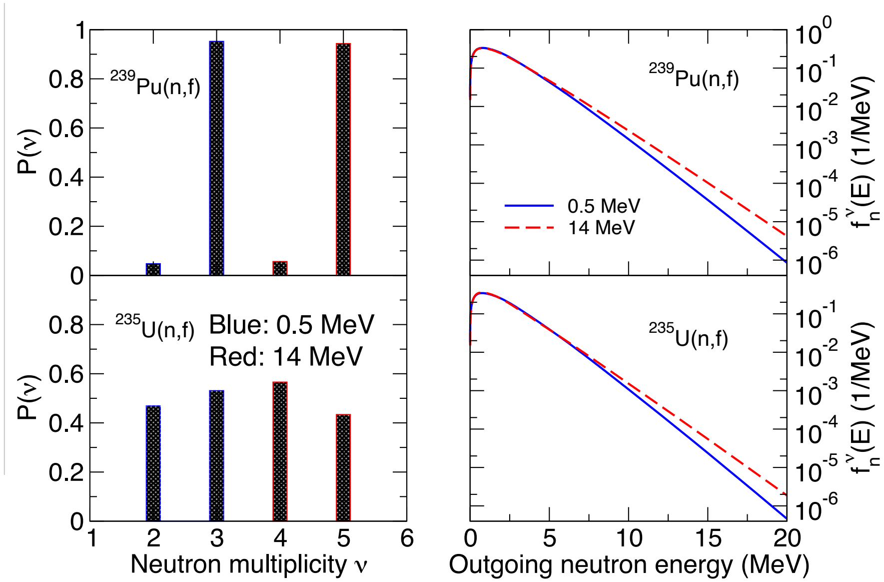

- In 'average' models, fission is a black box, neutron and gamma energies sampled from same average distribution, regardless of multiplicity and energy carried away by each emitted particle; fluctuations and correlations cannot be addressed

- Detailed models generate complete fission events: energy & momentum of neutrons, photons, and products in each individual fission event; correlations are automatically included

- Traditionally, neutron multiplicity sampled between nearest values to get correct average value
- All neutrons sampled from same spectral shape, independent of multiplicity – no conservation of energy or momentum!

Brief synopsis of how FREYA works

- For a given Z, A and energy ($E_n = 0$ for spontaneous fission), FREYA selects mass and charge of fragment from either data or a model (5 gaussian) parameterization
- Second fragment mass and charge obtained assuming binary fission, mass and charge conservation
- From fragment identities, fission Q value is obtained
- TKE(A_H) sampled from distribution; TXE obtained by energy conservation
- **'Spin temperature' sets level of rotational energy, remaining TXE given to intrinsic excitation energy**
- Intrinsic excitation divided between fragments, based on level densities, then thermal fluctuations introduced to obtain final excitation energy sharing
- Thermal fluctuations remove energy from TKE to maintain energy conservation, equivalent to width of TKE distribution
- **Spin fluctuations (conserving angular momentum), introduced for wriggling and bending modes**
- Pre-equilibrium emission and n-th chance fission included for $E_n \leq 20$ MeV
- After scission, fragments are de-excited first by emitting neutrons (Weisskopf-Ewing spectra) until the remaining energy is less than the neutron separation energy
- Photon emission follows until fragment no longer excited (statistical, then discrete emission)

FREYA has five physics-based parameters

- The fissioning nucleus, with A_0 nucleons, has an initial excitation energy E_{sc} including statistical and rotational excitation of the fragments
- The level density parameter, $a \sim A_0/e_0$, relates the temperature to the excitation energy, as in $E_{sc} = (A_0/e_0)\ T^2_{sc} - e_0$ is the first parameter
- **The fragment 'spin temperature' fluctuates around the scission temperature T_{sc} according to second parameter c_s, $T_s \sim c_s\ T_{sc}$, affecting rotational energy E_{rot} and photon observables**
- Total excitation energy, $E_{sc} = E_{rot} + E_{stat}$, E_{stat} is dissipated through neutron emission
- Statistical energy is partitioned between light and heavy fragments according to level density parameters, $E_{stat} = E^*_L + E^*_H$
- The light fragment energy is enhanced by third parameter, $x > 1$, by $E'^*_L = x\ E^*_L$ so that $E'^*_H = E_{stat} - E'^*_L$, affecting neutron multiplicity vs fragment mass
- Fragments get thermal variance, fourth parameter, c, controlling maximum available excitation and affecting neutron multiplicity distribution and moments
- Fifth parameter dTKE adjusts average TKE to fix average neutron multiplicity

Angular Momentum Generation in FREYA: based on nucleon exchange

Start from the rotating compound nucleus generated by the incoming neutron

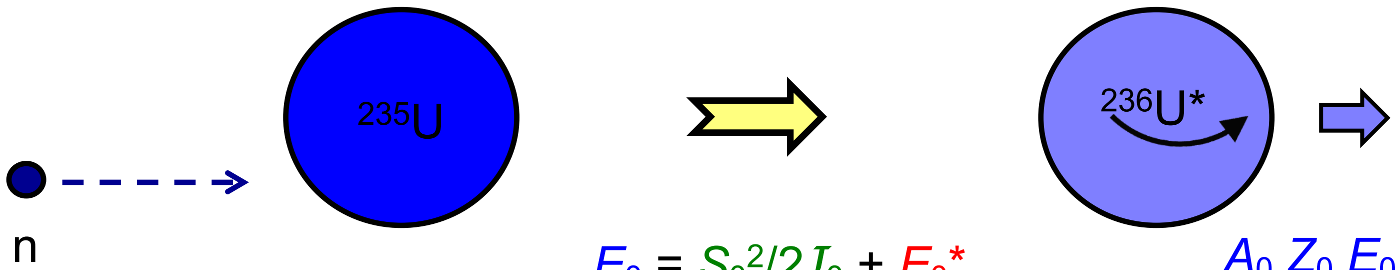

$A_0\ Z_0\ E_0\ \boldsymbol{S}_0\ \boldsymbol{P}_0$

$$E_0 = S_0^2/2\mathcal{I}_0 + E_0^*$$

Total initial excitation — Rotational energy — Statistical excitation

The plane of rotation is determined by the impact parameter of incident neutron; the plane may change due to *pre-fission neutron evaporation* (which is treated the same as the post-fission neutron evaporation from the rotating fragments)

Introduced (half) integer spin and can now specify fragments more precisely

RV & JR, PRC **103** (2021) 014610
JR & RV, PRL **127** (2021) 062502
JR, T. Dossing & RV, PRC **106** (2022) 014609
JR, PRC **106** (2022) L051601

FREYA mechanism of fragment spin generation: nucleon exchange

Relevant theory of nucleon exchange

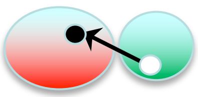

Damped heavy-ion collisions, W.U. Schröder and J.R. Huizenga, Ann. Rev. Nucl. Sci. (1977) 465

Intimate relationship between nucleon exchange and energy dissipation

Theory of transfer-induced transport in nuclear collisions, J. Randrup, Nucl. Phys. **A327** (1979) 490:

Each transfer changes the nucleon numbers and the excitation energies of the fragments, as well as their linear & angular momenta

Transport of angular momentum in damped nuclear reactions, J. Randrup, Nucl. Phys. **A383** (1982) 468:

Mobility (friction) tensor: anisotropic

*Dynamical evolution of angular momentum in damped nuclear reac*tions, T. Døssing and J. Randrup, Nucl. Phys. **A433** (1985) 215:

Relaxation times $t_{\text{wriggling}} << t_{\text{bending}}$ & $t_{\text{twisting}} <<< t_{\text{tilting}}$

fast ... slow

Expectations based on the *Nucleon Exchange Transport* model

Z_H, N_H, $\boldsymbol{P}_H$, $\boldsymbol{S}_H$, T_H,
Z_L, N_L, $\boldsymbol{P}_L$, $\boldsymbol{S}_L$, T_L

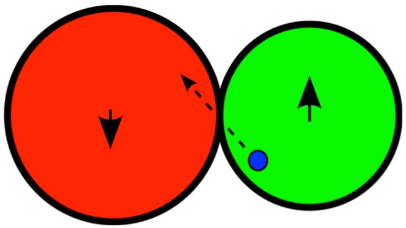

J. Randrup, Nucl. Phys. A **327**, 490 (1979)
J. Randrup, Nucl. Phys. A **383**, 468 (1983)
T. Døssing & J. Randrup, NPA **433**, 215 (1985)

Multiple nucleon transfers produce a dissipative force that affects the linear and angular momenta of the binary partners

Time scale:

The *mobility coefficients* for the rotational modes:

$$\begin{cases} M_{\rm wrig} = m\mathcal{N}R^2 \\ M_{\rm bend} = m\mathcal{N}\left[\left(\frac{\mathcal{I}_H R_L - \mathcal{I}_L R_H}{\mathcal{I}_L + \mathcal{I}_H}\right)^2 + c_{\rm ave}^2\right] \\ M_{\rm twst} = m\mathcal{N}c_{\rm ave}^2 \end{cases}$$

One-way nucleon current: $\mathcal{N} \approx \frac{1}{4}\rho\bar{v}\pi c^2 \quad (\bar{v} \doteq \frac{3}{4}v_F \quad)$

Center separation: $R = R_L + R_H + d$

Neck radius: $c \quad (c^2 \ll R^2 \quad)$

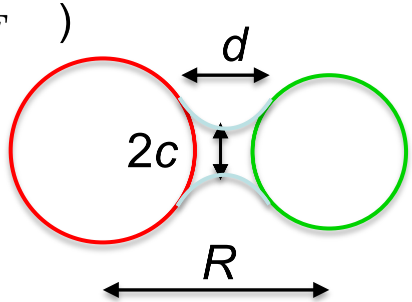

Basic Kinematic Setup

Two moving particles

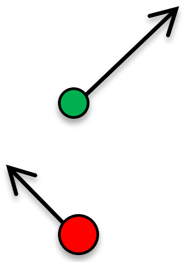

$\boldsymbol{p}_1 = m_1 \boldsymbol{v}_1$ $\quad \boldsymbol{P} = \boldsymbol{p}_1 + \boldsymbol{p}_2 = M\boldsymbol{V} = \boldsymbol{p}_+$ $\quad m_+ = M = m_1 + m_2$ ***TOTAL***

$\boldsymbol{p}_2 = m_2 \boldsymbol{v}_2$ $\quad \boldsymbol{p} = \mu(\boldsymbol{v}_1 - \boldsymbol{v}_2) = \mu \boldsymbol{v} = \boldsymbol{p}_-$ $\quad \frac{1}{m_-} = \frac{1}{\mu} = \frac{1}{m_1} + \frac{1}{m_2}$ ***RELATIVE***

$$E_{\mathrm{kin}} = \frac{p_1^2}{2m_1} + \frac{p_2^2}{2m_2} = \frac{P^2}{2M} + \frac{p^2}{2\mu} = \frac{p_+^2}{2m_+} + \frac{p_-^2}{2m_-}$$

Two rotating spheres

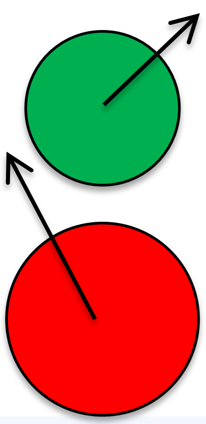

$\boldsymbol{S}_1 = I_1 \omega_1$ $\quad \boldsymbol{S} = \boldsymbol{S}_1 + \boldsymbol{S}_2 = \boldsymbol{s}_+$ $\quad I_+ = I_{\mathrm{tot}} = I_1 + I_2$ ***TOTAL***

$\boldsymbol{S}_2 = I_2 \omega_2$ $\quad \boldsymbol{s} = I_{\mathrm{rel}}(\omega_1 - \omega_2) = \boldsymbol{s}_-$ $\quad \frac{1}{I_-} = \frac{1}{I_{\mathrm{rel}}} = \frac{1}{I_1} + \frac{1}{I_2}$ ***RELATIVE***

$$E_{\mathrm{rot}} = \frac{S_1^2}{2\mathcal{I}_1} + \frac{S_2^2}{2\mathcal{I}_2} = \frac{s_+^2}{2\mathcal{I}_+} + \frac{s_-^2}{2\mathcal{I}_-}$$

Angular momentum after scission

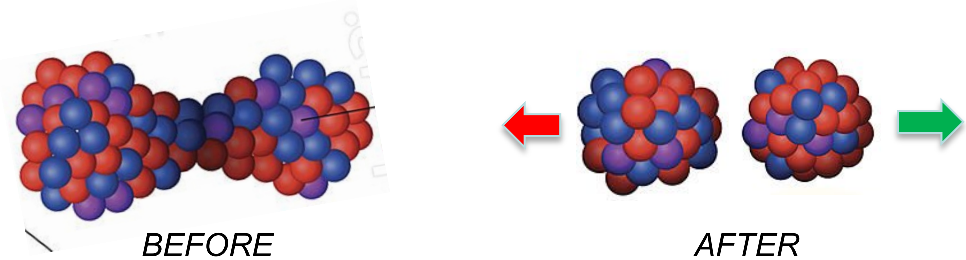

Three *coupled* angular momenta:

- Spin of the light fragment $\boldsymbol{S}_L$
- Spin of the heavy fragment $\boldsymbol{S}_H$
- Orbital angular momentum $\boldsymbol{L}$

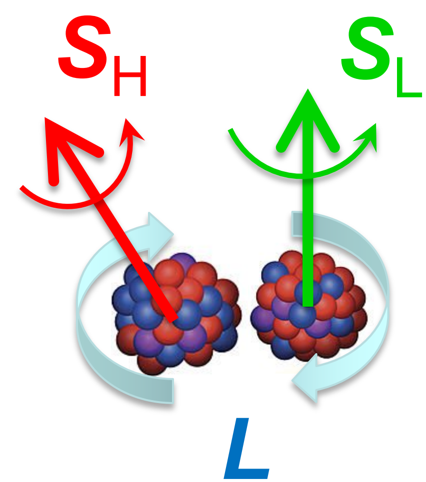

The total angular momentum is *conserved*:

$$\boldsymbol{S}_L + \boldsymbol{S}_H + \boldsymbol{L} = \boldsymbol{S}_0 \ (\approx \mathbf{0} \text{ for spontaneous fission})$$

=> *Six* independent internal rotational modes

Rotational modes of the two-fragment system

J.R. Nix & W.J. Swiatecki,
Nucl. Phys. **71**, 1 (1963):

	#				
+ +	2	*Wriggling:*	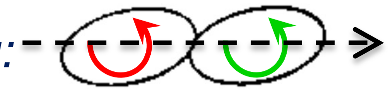	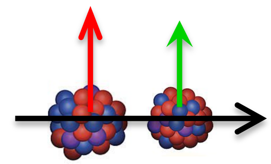	mutually parallel, perpendicular to axis
- -	2	*Bending:*	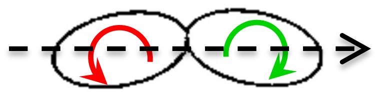	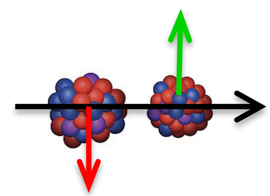	mutually anti-parallel, perpendicular to axis
+	1	*Tilting:*	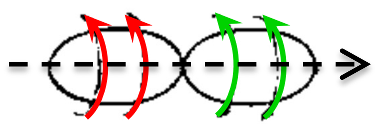	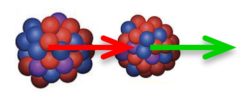	mutually parallel, parallel to axis
-	1	*Twisting:*	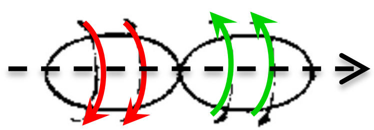	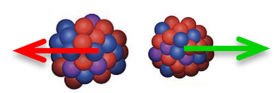	mutually anti-parallel, parallel to axis

Added to FREYA in 2014

Rotational modes in dinuclear complex: damped nuclear reactions

$$\boldsymbol{S}_0 = \boldsymbol{S}_L + \boldsymbol{S}_H + \boldsymbol{L}$$

$$E_0^{\mathrm{rot}} = \frac{S_L^2}{2\mathcal{I}_L} + \frac{S_H^2}{2\mathcal{I}_H} + \frac{(\boldsymbol{S}_0 - \boldsymbol{S}_L - \boldsymbol{S}_H)^2}{2\mathcal{I}_R}$$
$$= \frac{S_0^2}{2\mathcal{I}_0} + \frac{s_{\mathrm{wrig}}^2}{2\mathcal{I}_{\mathrm{wrig}}} + \frac{s_{\mathrm{bend}}^2}{2\mathcal{I}_{\mathrm{bend}}} + \frac{s_{\mathrm{twst}}^2}{2\mathcal{I}_{\mathrm{twst}}} + \frac{s_{\mathrm{tilt}}^2}{2\mathcal{I}_{\mathrm{tilt}}}$$

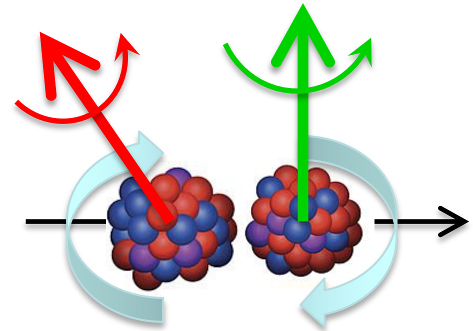

2 *Wriggling:*

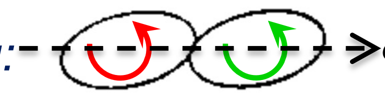

$$\delta \boldsymbol{S}_{L,H}^{\mathrm{wrig}} = \frac{\mathcal{I}_{L,H}}{\mathcal{I}_L + \mathcal{I}_H} \boldsymbol{s}_{\mathrm{wrig}} \,, \quad \delta \boldsymbol{L}^{\mathrm{wrig}} = -\boldsymbol{s}_{\mathrm{wrig}}$$

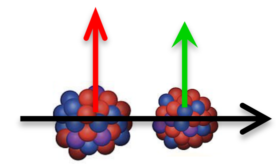

2 *Bending:*

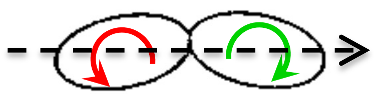

$$\delta \boldsymbol{S}_L^{\mathrm{bend}} = \boldsymbol{s}_{\mathrm{bend}} \,, \quad \delta \boldsymbol{S}_H^{\mathrm{bend}} = -\boldsymbol{s}_{\mathrm{bend}} \,, \quad \delta \boldsymbol{L}^{\mathrm{bend}} = \boldsymbol{0}$$

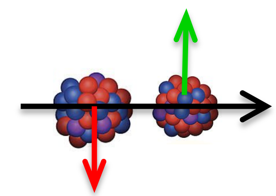

1 *Twisting:*

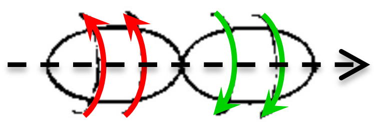

$$\delta \boldsymbol{S}_L^{\mathrm{twst}} = \boldsymbol{s}_{\mathrm{twst}} \,, \quad \delta \boldsymbol{S}_H^{\mathrm{twst}} = -\boldsymbol{s}_{\mathrm{twst}} \,, \quad \delta \boldsymbol{L}^{\mathrm{twst}} = \boldsymbol{0}$$

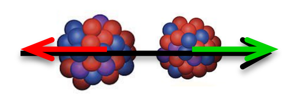

1 *Tilting:*

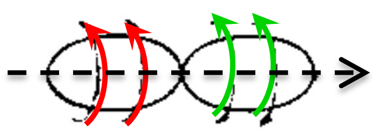

is not directly agitated in because $\boldsymbol{L} \cdot \boldsymbol{R} = 0$

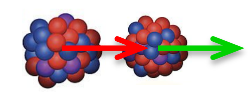

Total angular momentum still conserved

FREYA can be used to explore different scenarios:

In order to explore a variety of rotational scenarios, we the introduce the *mode temperatures* $T_m = c_m T_{sc}$

The mode amplitudes $\{s_m\}$ are thus sampled from

Mode spins:

$$P_{\rm wrig}(s_{\rm wrig}) \sim \exp(-s_{\rm wrig}^2/2\mathcal{I}_{\rm wrig}T_{\rm wrig})\,, \quad T_{\rm wrig} = c_{\rm wrig}T_{\rm sc}$$

$$P_{\rm bend}(s_{\rm bend}) \sim \exp(-s_{\rm bend}^2/2\mathcal{I}_{\rm bend}T_{\rm bend})\,, \quad T_{\rm bend} = c_{\rm bend}T_{\rm sc}$$

$$P_{\rm twst}(s_{\rm twst}) \sim \exp(-s_{\rm twst}^2/2\mathcal{I}_{\rm twst}T_{\rm twst})\,, \quad T_{\rm twst} = c_{\rm twst}T_{\rm sc}$$

Fragment spins:

$$\Rightarrow \begin{cases} \mathbf{S}_L = (\mathcal{I}_L/\mathcal{I}_+)\,\mathbf{s}_{\rm wrig} + \mathbf{s}_{\rm bend} + \mathbf{s}_{\rm twst} \\ \mathbf{S}_H = (\mathcal{I}_H/\mathcal{I}_+)\,\mathbf{s}_{\rm wrig} - \mathbf{s}_{\rm bend} - \mathbf{s}_{\rm twst} \end{cases}$$

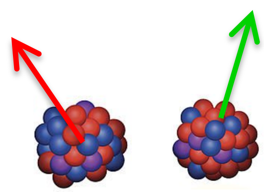

The relative presence of the different modes *m* can then be tuned by the coefficients ($c_{\rm wrig}$, $c_{\rm bend}$, $c_{\rm twst}$)

Example: Standard FREYA → (1,1,0): full wriggling & bending, no twisting

Relaxation times of dinuclear rotational modes

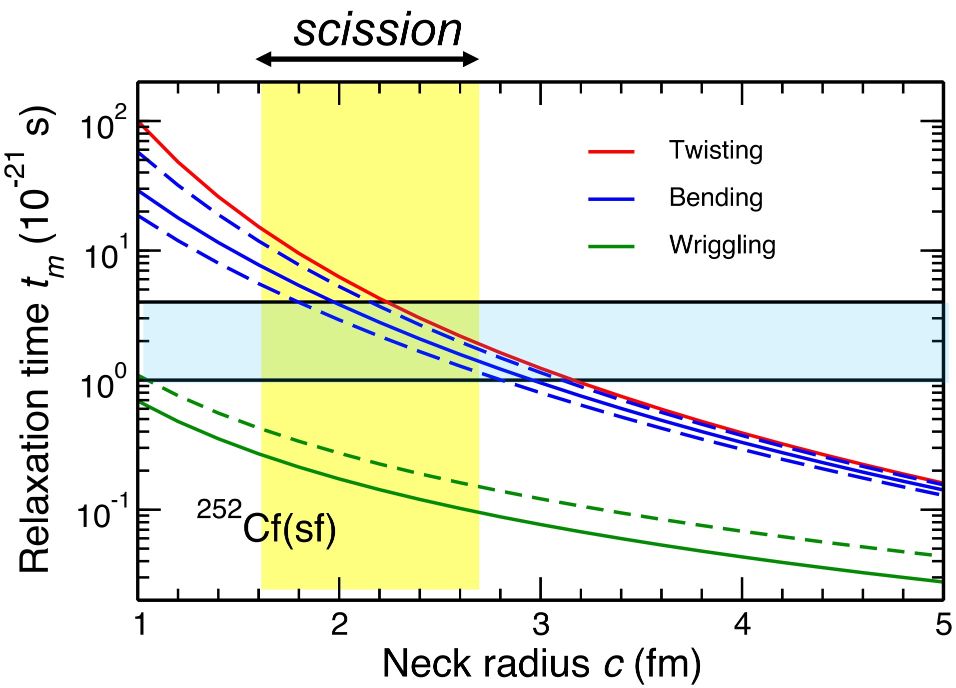

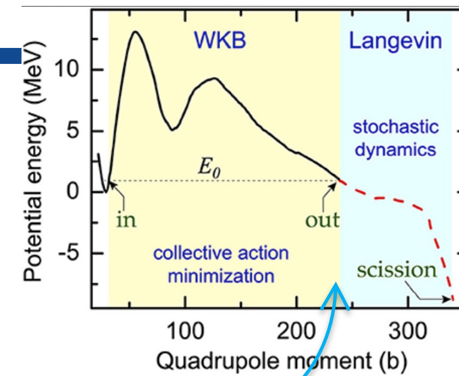

t_{fiss} : *fission time* ≈ 1 - 4 10^{-21} s

Expectations from nucleon exchange:

- *Wriggling* is probably fully agitated
- *Twisting* is unlikely to play a major role; it grows more prominent with excitation
- *Bending* probably has some presence; it increases with the mass asymmetry

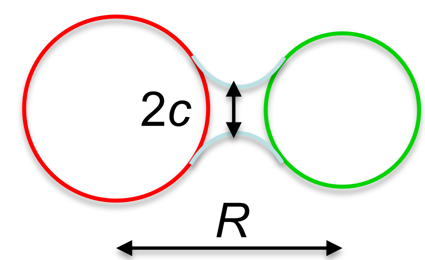

Neutron evaporation from rotating fragments

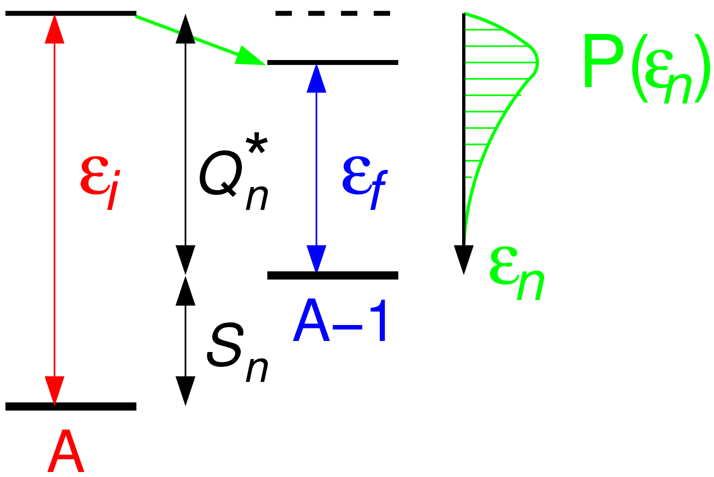

$$M_i^* = M_i^{\rm gs} + \varepsilon_i \qquad M_f^* = M_f^{\rm gs} + \varepsilon_f \qquad M_i^* = M_f^* + m_{\rm n} + \epsilon$$

$$Q_{\rm n} \equiv Q_{\rm n}^*(\varepsilon_i = 0) = M_i^{\rm gs} - M_f^{\rm gs} - m_{\rm n} = -S_{\rm n}$$

$$Q_{\rm n}^* = \varepsilon_i + Q_{\rm n} = \varepsilon_i - S_{\rm n}$$

$$\epsilon + \varepsilon_f = M_i^* - M_f^{\rm gs} - m_{\rm n} = Q_{\rm n}^* = \begin{cases} \varepsilon_f^{\rm max} \\ \epsilon^{\rm max} \end{cases}$$

$$T_f^{\rm max} = \sqrt{\varepsilon_f^{\rm max}/a_f} = \sqrt{Q_{\rm n}^*/a_f}$$

Weisskopf-Ewing neutron energy spectrum: $d^3\boldsymbol{p} \sim \sqrt{\epsilon}\, d\epsilon\, d\Omega$ *(non-relativistic)*

$$\frac{d^3N}{d^3\boldsymbol{p}} d^3\boldsymbol{p} \sim \sqrt{\epsilon}\, {\rm e}^{-\epsilon/T_f^{\rm max}} \sqrt{\epsilon}\, d\epsilon\, d\Omega = {\rm e}^{-\epsilon/T_f^{\rm max}} \epsilon\, d\epsilon\, d\Omega$$

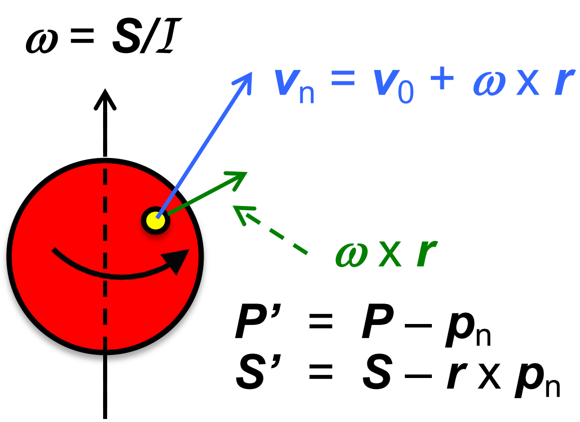

When fragment is rotating, emission from moving surface, v_0, is boosted by local rotational velocity $\boldsymbol{\omega} \times \boldsymbol{r}$ and daughter nucleus absorbs recoil linear and angular momentum

Neutron and daughter nucleus Lorentz boosted from emitter frame to laboratory frame

Neutron emission conserves energy and linear & angular momentum

Photon emission follows neutron emission

Neutron evaporation ceases when $E^* < S_n$ (neutron separation energy); the remaining excitation energy is disposed of by sequential photon emission …

… first by statistical photon cascades down to the yrast line …

$$\frac{d^3N}{d^3\mathbf{p}_\gamma} d^3\mathbf{p}_\gamma \sim \left[\frac{\Gamma^2_{\rm GDR}\epsilon^2}{(\epsilon^2-\epsilon_{\rm GDR^2})^2+\Gamma^2_{\rm GDR}\epsilon^2}\right]\epsilon^2 e^{-\epsilon/T_i} \quad \Leftarrow \quad d^3\boldsymbol{p}_\gamma \sim \epsilon^2 d\epsilon\, d\Omega$$

(ultrarelativistic)

$S_f = S_i - 1$

$$E^*_f = E^*_i - \epsilon_\gamma \qquad \epsilon_{\rm GDR} = \left(31.2A^{-1/3} + 20.6A^{-1/6}\right)\ {\rm MeV} \qquad \Gamma_{\rm GDR} = 5\ {\rm MeV}$$

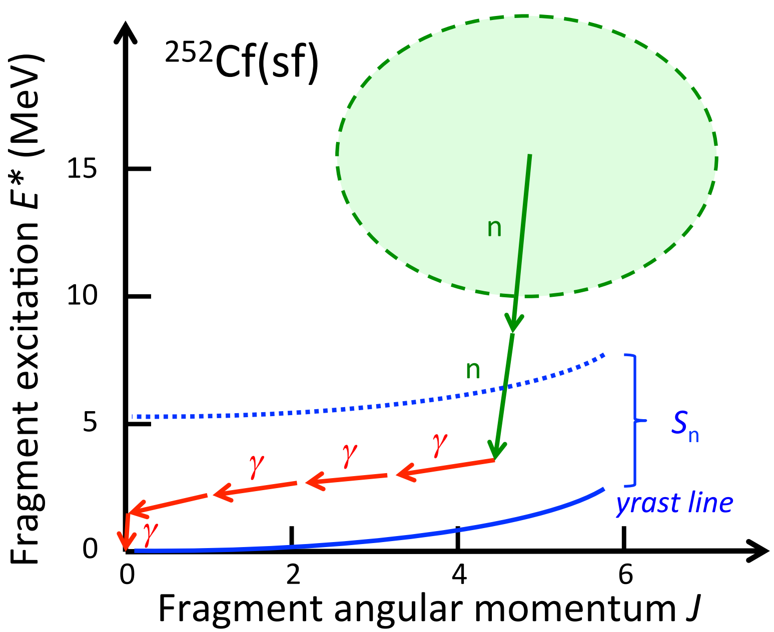

.. then by stretched E2 photons along the yrast line …

$$S_f = S_i - 2$$
$$\epsilon_\gamma = S_i^2/2\mathcal{I}_A - S_f^2/2\mathcal{I}_A$$
$$\mathcal{I}_A = 0.5 \times \tfrac{2}{5} A m_N R_A^2$$

… whenever possible, the RIPL decay tables are used instead…

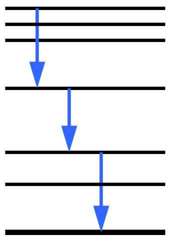

Each photon is Lorentz boosted from the emitter to the laboratory frame

How can we learn about angular momentum based on measurements?

Recent experimental information on spin correlations

Angular momentum generation in nuclear fission,
J. N. Wilson *et al.*, Nature **590** (2021) 566

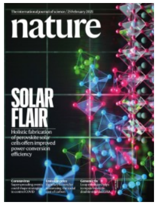

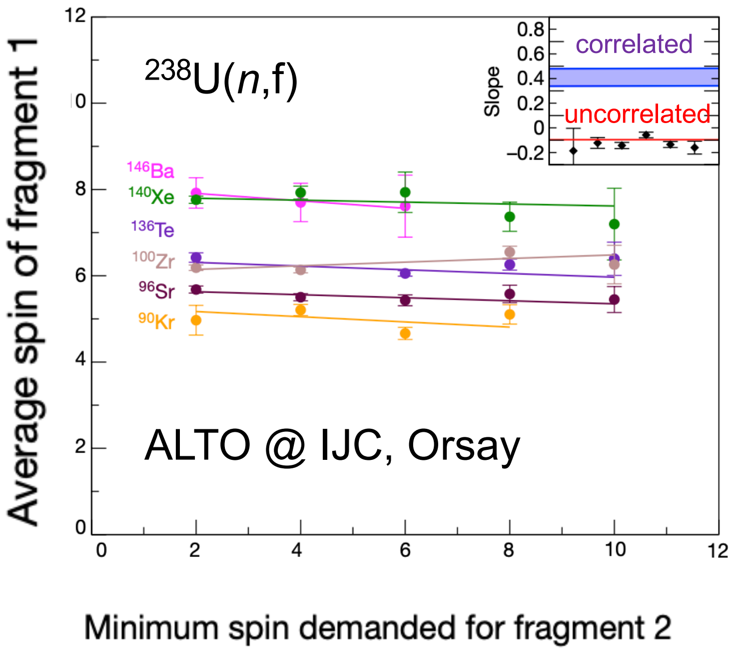

OBSERVATION:

``There is no significant correlation between the spins of the fragments"

INTERPRETATION:

Therefore ``the fragment spins are generated after the nucleus splits", i.e. ``after the fragments have become two separate, independent systems"

Dominance of fluctuations results in very weak fragment spin correlation

- The fragment spins $\boldsymbol{S}_L$ & $\boldsymbol{S}_H$ are dominated by wriggling & bending fluctuations and are only very weakly correlated (both mutually and w.r.t $\boldsymbol{S}_0$)
- Recoil from wriggling creates some orbital motion and the subsequent Coulomb trajectory reorients the direction of the relative fragment motion by about 2°
- The remaining weak directional correlation is effectively independent of the initial energy, the compound nuclear spin, and the fragment mass division
- There is a slight preference for opposite spin directions: $P(180°)/P(0°) = 1.18$

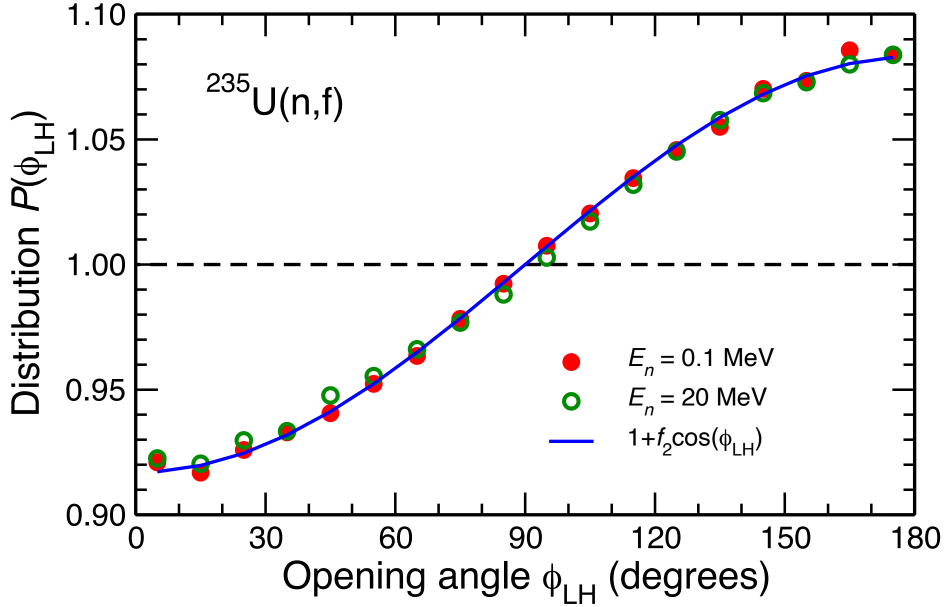

R.V. and J. Randrup, PRC **103** (2021) 014610

Moment of inertia for orbital motion is large: $I_R \gg I_H, I_L \rightarrow$ very weak fragment spin correlations

We can calculate the direction and magnitude of spin correlations

spin-spin correlation coefficient:

$$c(\boldsymbol{S}_L, \boldsymbol{S}_H) \equiv \frac{\langle \delta\boldsymbol{S}_L \cdot \delta\boldsymbol{S}_H \rangle}{[\langle \delta S_L^2 \rangle \langle \delta S_H^2 \rangle]^{1/2}} = -\left[\frac{\mathcal{I}_L \qquad \mathcal{I}_H}{(\mathcal{I}_R + \mathcal{I}_L)(\mathcal{I}_R + \mathcal{I}_H)}\right]^{\frac{1}{2}} \ll 1$$

Correlation between the spin *directions*:

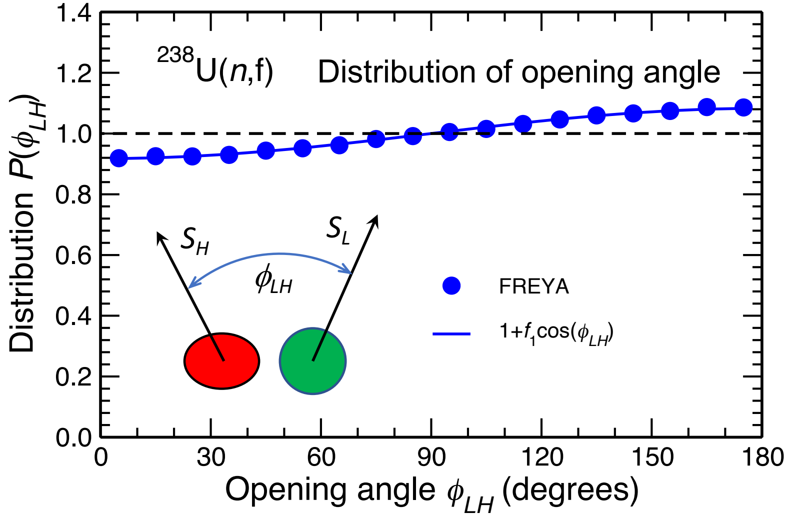

Correlation between the spin *magnitudes*:

Case:	^{235}U(n,f)	^{238}U(n,f)	^{239}Pu(n,f)	^{252}Cf(sf)
$\bar{S}_L = \langle S_L \rangle$	4.27	4.43	4,58	5.08
$\bar{S}_H = \langle S_H \rangle$	5.66	5.80	5.93	6.33
$c(S_L, S_H)$ (%)	0.2	0.2	0.1	0.1
f_1 (%)	−8.2	−8.3	−8.3	−8.4

magnitude of correlation coefficient:

$$c(S_L, S_H) \equiv \frac{\langle \delta S_L \delta S_H \rangle}{[\langle \delta S_L^2 \rangle \langle \delta S_H^2 \rangle]^{1/2}}$$

JR & RV, PRL **127** (2021) 062502, RV & JR, PRC **103** (2021) 014610

Neutron emission from rotating fragments causes angular anisotropy

- Neutron emission from a rotating fragment results in an equatorial bulge in the angular distribution due to centrifugal force
- The bulge is practically independent of the initial compound spin
- The resulting *dynamical anisotropy* can be expressed by $A = dN_n/d\Omega_{nS}(90^o)/dN_n/d\Omega_{nS}(0) - 1 = 0.093$ (consistent with observations – Vorobyev)
- The evaporation chains reorient the fragment spins by 13^o on average but change the spin magnitudes only slightly, by $0.06\hbar$

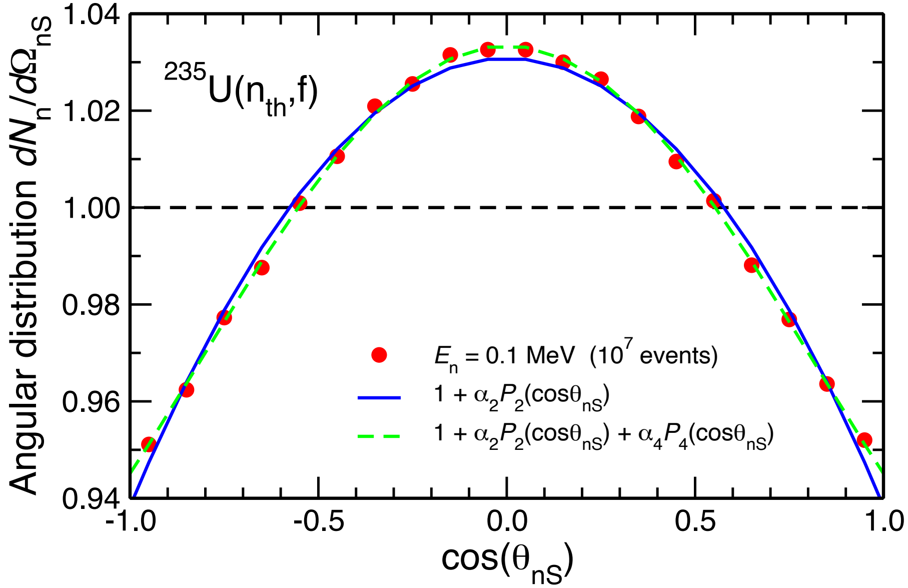

R.V. and J. Randrup, PRC **103** (2021) 014610

Wilson et al. also measured fragment spins:

Nature **590** (2021) 566

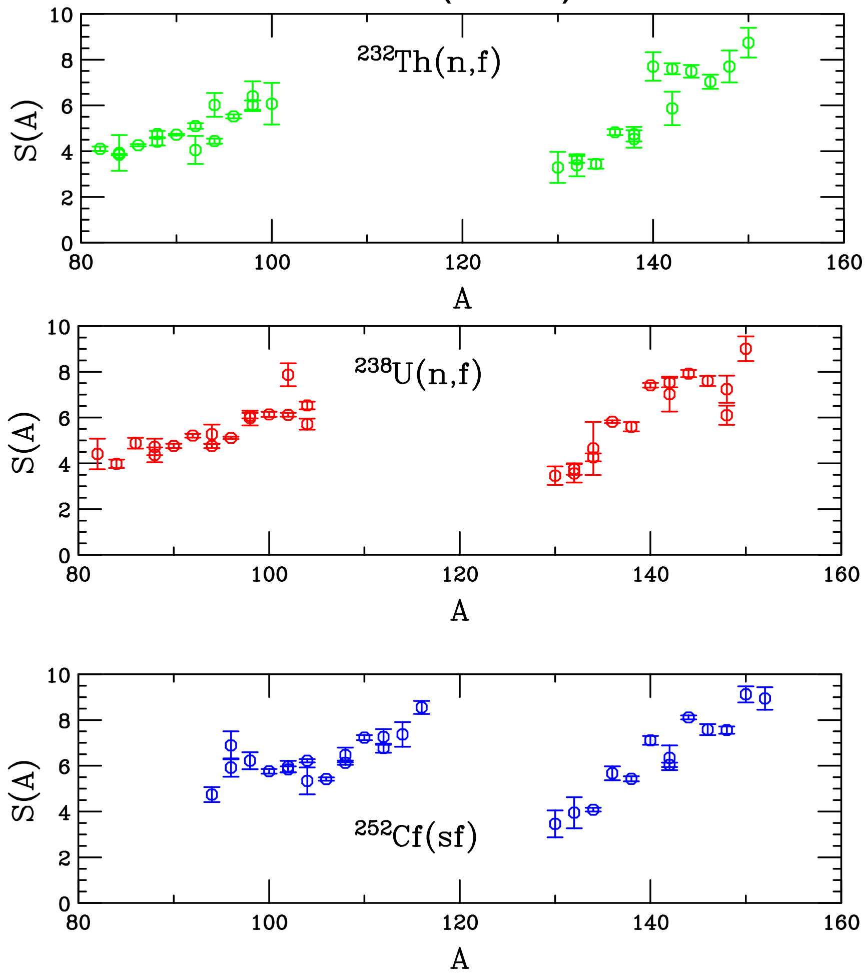

Measured S(A) is sawtooth-like, similar to ν(A), and, possibly, ν_γ(A) although new measurements should be made to confirm this behavior

We can model S(A) of the fragments & compare to data

Default moments of Inertia in FREYA have a simple dependence on mass:

$$\mathcal{I}_L \;\alpha\; (1/2)M_L R_L^2 \qquad \mathcal{I}_H \;\alpha\; (1/2)M_H R_H^2$$

This simple dependence means that S(A) has a weak dependence on A

If the default moments of inertia are replaced by moments of inertia that schematically depend on the ground state deformation of the fragments,

$$I'_f(A_f) = 0.2[I_{rig}(A_f;0) + 10(I_{rig}(A_f;\varepsilon(A_f)) - I_{rig}(A_f;0))],$$

where ε is obtained from a fit to the ground state deformations

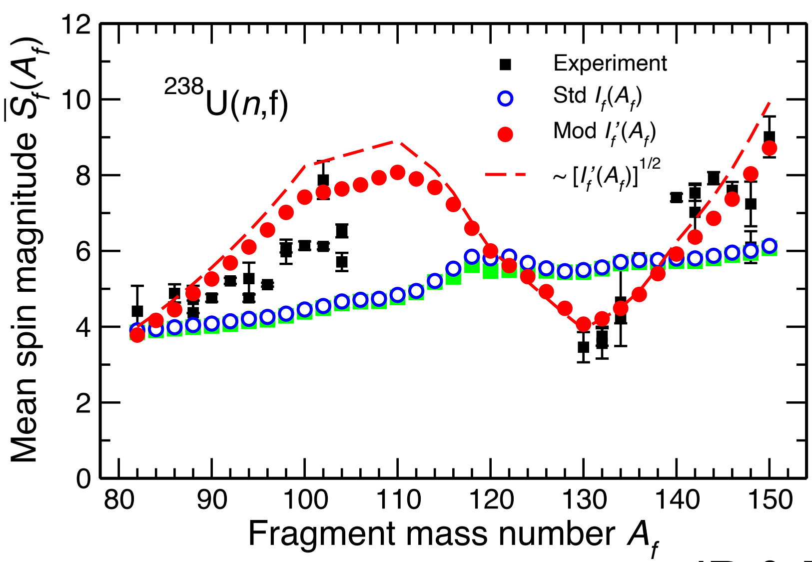

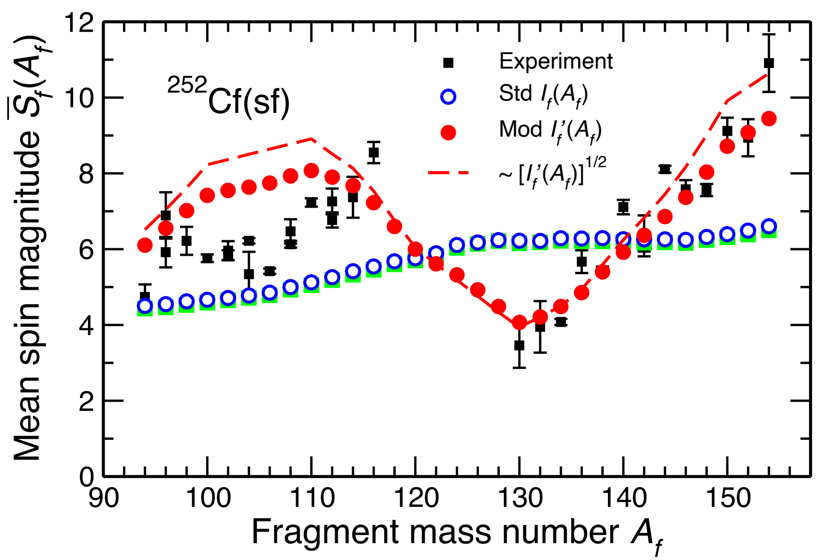

JR & RV, PRL **127** (2021) 062502

How can we differentiate between different levels of spin fluctuations?

Probing fragment spin directions and thus spin modes using photon measurements

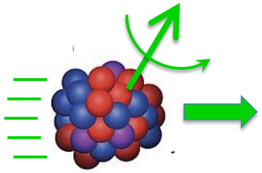

Orientation of the fragment spins relative to the fragment motion?

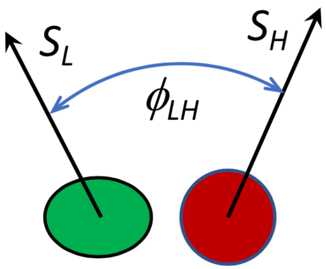

Relative orientation of the fragment spins?

JR, T Dossing & RV, PRC **106** (2022) 014609

Angular distribution relative to fragment direction $dN/d\cos(\theta_{\gamma,f})$

Look only at E2 emissions in *even-even* product nuclei

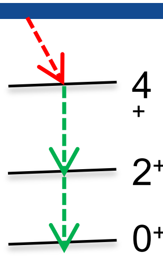

Pioneering experiments:
J.B. Wilhelmy *et al.*, Phys. Rev. C **5**, 2041 (1972)
A. Wolf & E. Cheifetz, Phys. Rev. C **13,** 1952 (1976)

Two reference scenarios:

The fragment spin is *parallel* to the direction of motion:

$$W_{\|}(\theta_{\gamma f}) \sim 1 - \tfrac{5}{7}P_2(\cos\theta_{\gamma f}) - \tfrac{2}{7}P_4(\cos\theta_{\gamma f})$$

Fragment spin is *perpendicula* to the direction of motion:

$$W_{\perp}(\theta_{\gamma f}) \sim 1 + \tfrac{5}{14}P_2(\cos\theta_{\gamma f}) - \tfrac{3}{28}P_4(\cos\theta_{\gamma f})$$

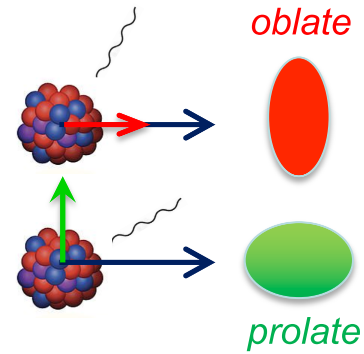

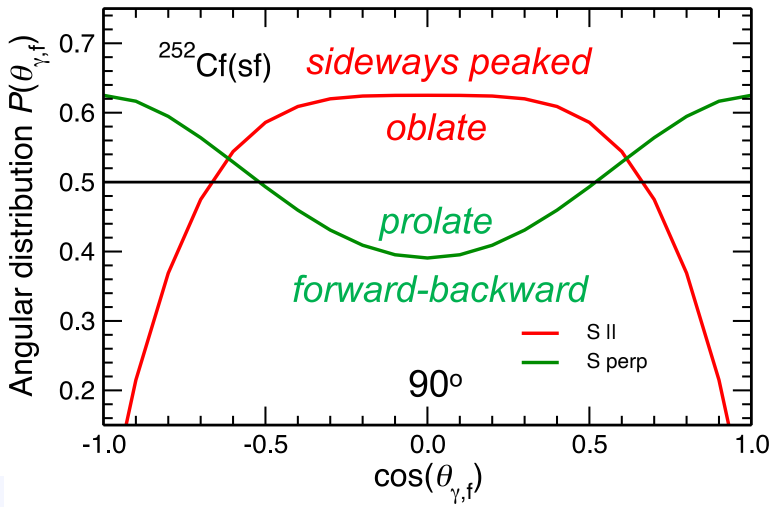

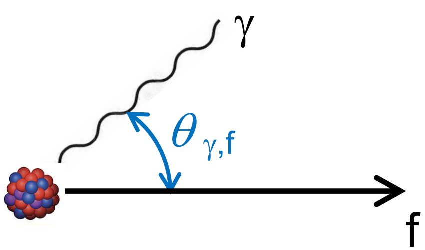

Testing different contributions from twisting mode

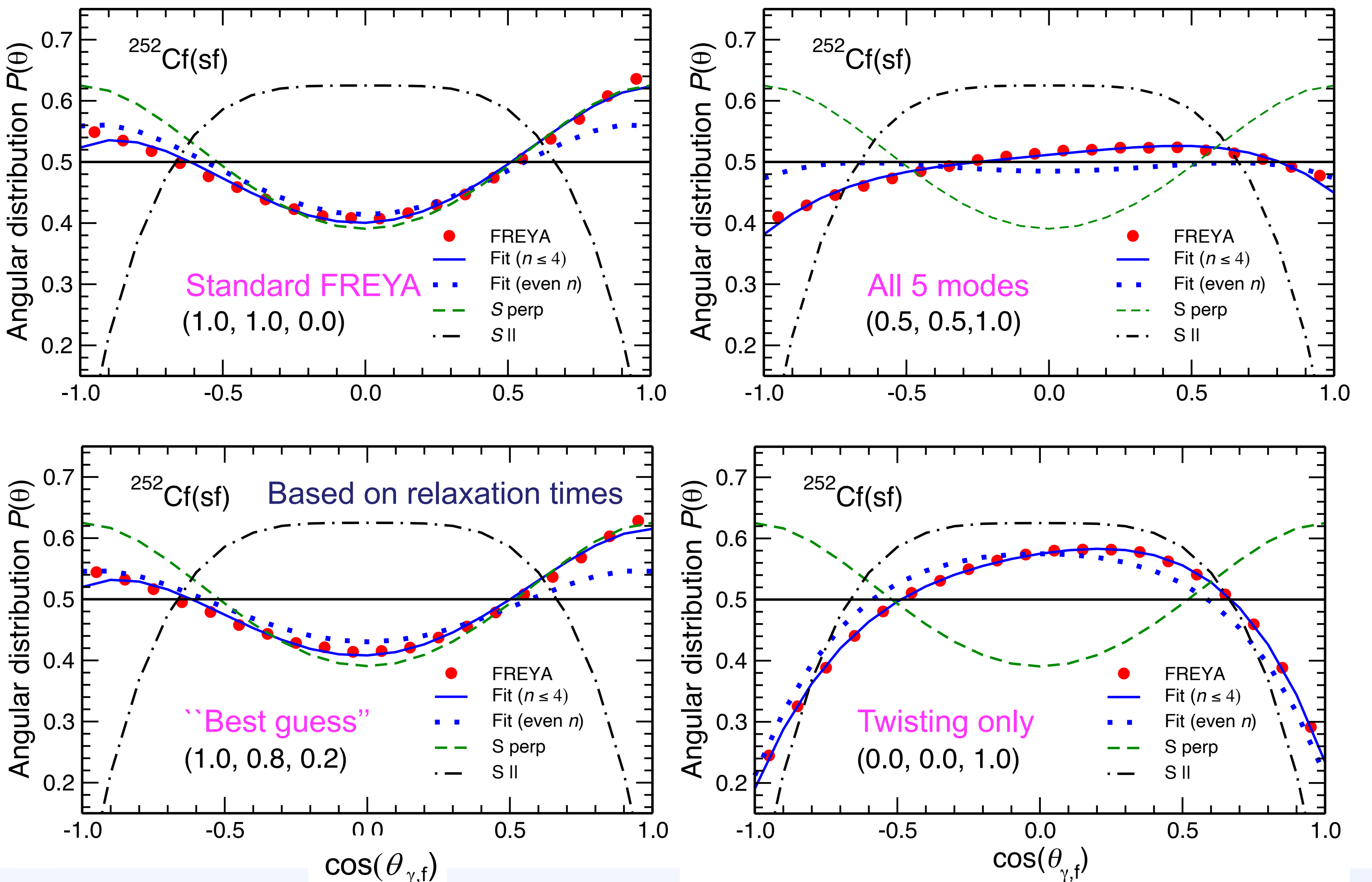

Yields at 0° relative to yield at 90° adding more twisting

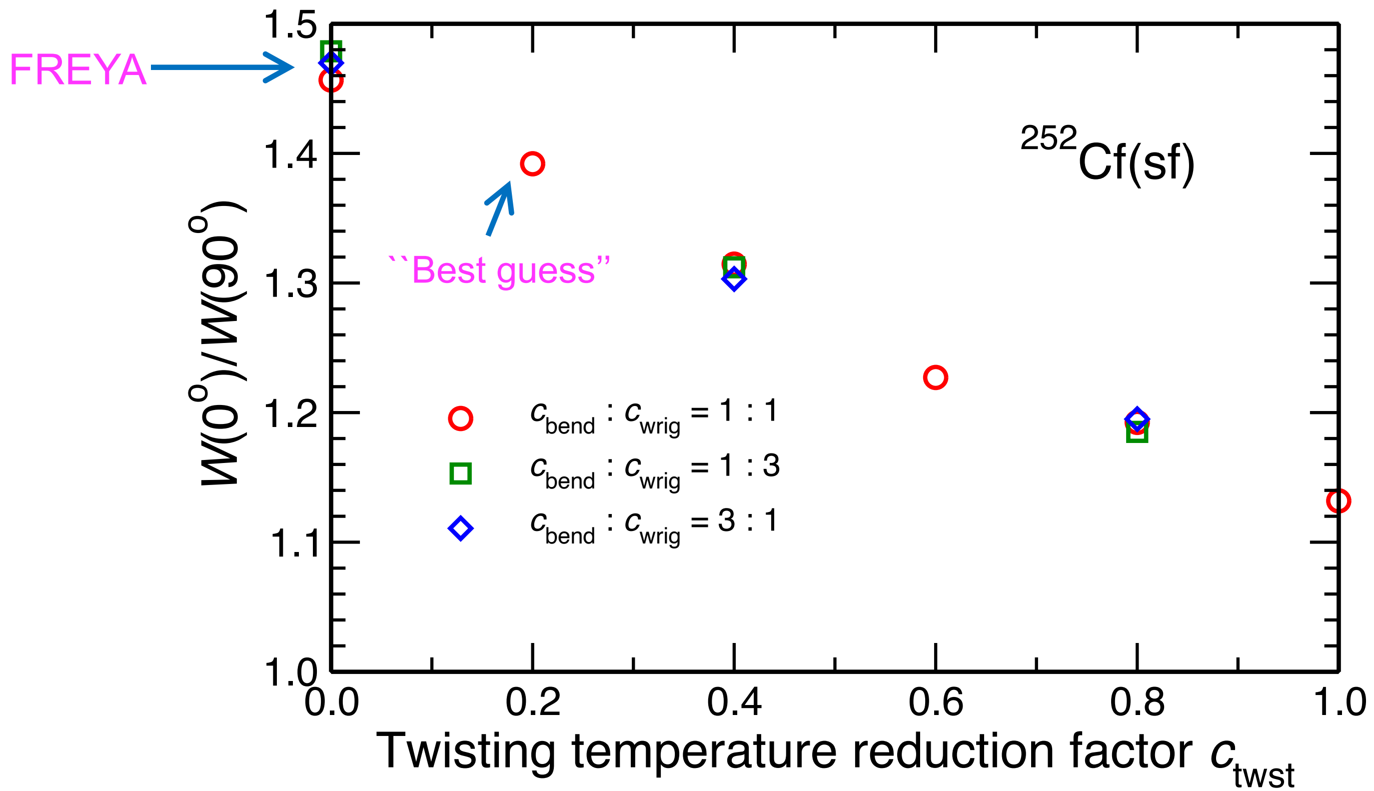

Repeat the experiment by Wilhelmy *et al.:*
Modern equipment => more accurate data
=> measure the degree of ***twisting***

Correlation between the two fragment spin *directions*?

A photon having *positive* helicity tends to emerge in the *upper* hemisphere

$$P_{2,h}^{E2}(\theta_{\gamma S}) \ \sim \ \tfrac{1}{4}(1 + h\cos\theta_{\gamma S})^2(1 - \cos^2\theta_{\gamma S})$$

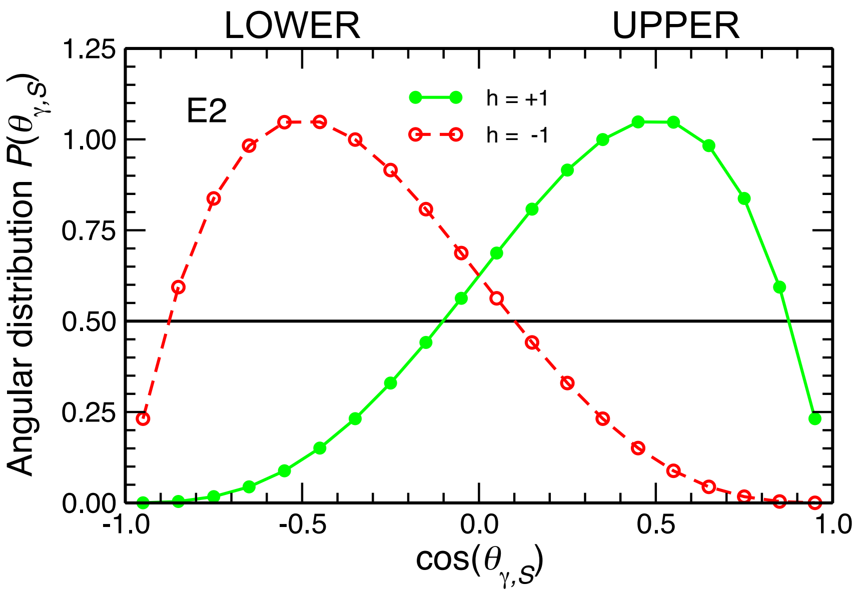

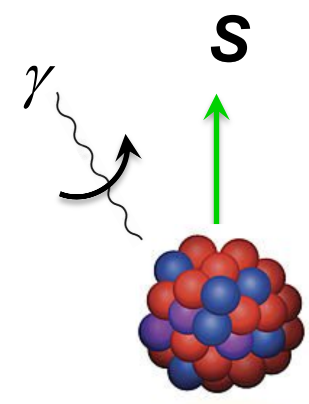

$$dN_i/d\cos\theta_i \ = \ \sum_{n\geq 0}\alpha_n^{(i)}P_n(\cos\theta_i) \quad \Rightarrow \quad P(\psi_{12}) = 2\sum_{n\geq 0}\frac{\alpha_n^{(1)}\alpha_n^{(2)}}{2n+1}P_n(\cos\psi_{12})$$

Measure the distribution of the opening angle ψ_{12} between two E2 photons with identified *helicities* originating from partner fragments

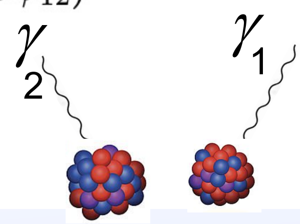

Distribution of the opening angle between two E2 photons having the *same* helicity

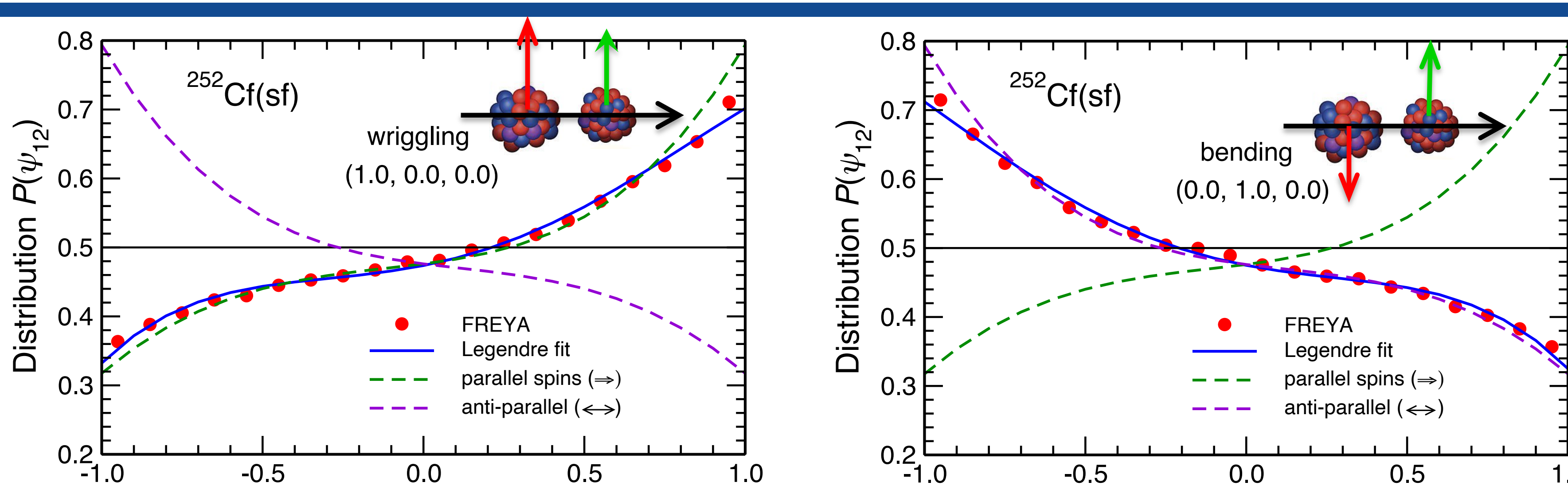

Wriggling: same hemisphere, small angle

Bending: opposite hemisphere,large angle

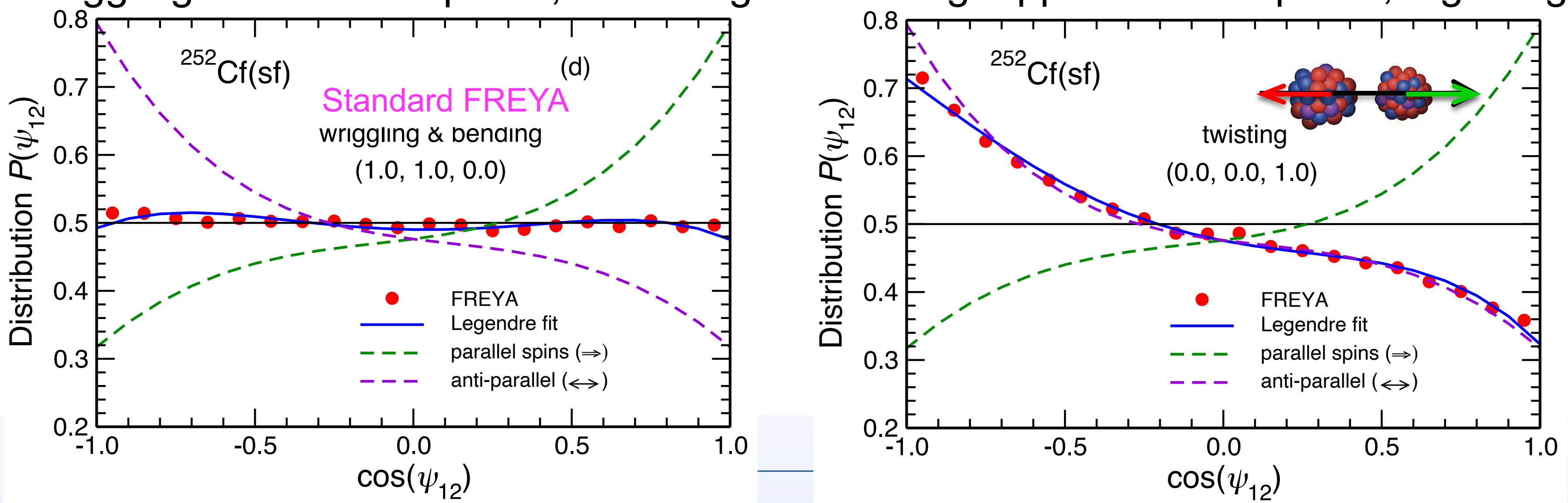

Summary

- Angular momentum has been a hot topic in fission for more than 60 years
- Experiment suggests that fission fragments typically carry S = 5-7$\hbar$, approximately directed perpendicular to the fission axis
- Because FREYA conserves energy, linear & angular momentum, it can straightforwardly elucidate the influence of angular momentum
- We have studied the influence of the overall angular momentum and showed that the two fragment spins are nearly uncorrelated even though they are built up in highly correlated increments (by nucleon exchange)
- Fragment rotation has numerous consequences, it:
  - causes neutron emission to be anisotropic;
  - influences photon emission;
  - affects searches for novel effects like scission neutrons
- Spin-spin correlations can provide information on the scission geometry

FREYA is ideal for studying spin effects in fission

FREYA references

- **FREYA** developed in collaboration with J. Randrup (LBNL); neutron-transport code integration by J. Verbeke (LLNL); available in MCNP6.2
- **FREYA** journal publications: Phys. Rev. C **80** (2009) 024601, 044611; **84** (2011) 044621; **85** (2012) 024608; **87** (2013) 044602; **89** (2014) 044601; **90** (2014) 064623; **96** (2017) 064620; **99** (2019) 054619; **103** (2021) 014610; Phys. Rev. Lett. **127** (2021) 062502;
- Parameter optimization for spontaneous fission: NIM A **922** (2019) 36
- **FREYA** published in Comp. Phys. Comm. **191** (2015) 178; **222** (2018) 263.
- "Nuclear Fission", Chapter 5 of '100 Years of Subatomic Physics', World Scientific, 2013
- Review in Eur. Phys. J. A **54** (2018) 9
- Papers with experimentalists: neutron polarization in photofission: Mueller *et al,* Phys. Rev. C **89** (2014) 034615; photon production: Gjerstvang *et al.,* Phys. Rev. C **103** (2021) 034609; neutron-gamma correlations: Wang *et al*, Phys. Rev. C **93** (2016) 014606, Marcath *et al*, Phys. Rev. C **97** (2018) 044622, Marin et al, NIM A **968** (2020) 163907 , PRC **104** (2021) 024602; neutron-neutron correlations, Schuster et al, Phys. Rev. C **100** (2019) 014605; Verbeke *et al*, Phys. Rev. C **97** (2018) 044601; Pozzi *et al,* Nucl. Sci. Eng. **178** (2014) 250.
- Fission in Astrophysics: Vassh *et al.,* J. Phys. G **46** (2019) 065202; Wang *et al.,* Ap. J. Lett. **903** (2020) L3
- Isotopes currently included: spontaneous fission of ^{252}Cf, ^{244}Cm, ^{238,240,242}Pu, ^{238}U and neutron-induced fission of ^{233,235,238}U(n,f), ^{239,241}Pu(n,f) for $E_n \leq 20$ MeV